

A Numerical Study on Pedestrian and Wheelchair User Safety in VRU-Vehicle Collisions

Niclas Trube, Patrick Matt, Matthias Boljen

I. INTRODUCTION

Road traffic crashes are the cause of 1.35 million deaths each year worldwide, almost half of which account for Vulnerable Road Users (VRUs) [1]. By definition, VRUs include persons with disabilities or reduced mobility and orientation, such as wheelchair users (WCUs), besides pedestrians and cyclists. However, users of non-motorised wheelchairs and motorised mobility aids are rarely mentioned in statistics [2].

Available data allows the following statements. WCUs have a 36 % higher mortality rate than the overall population of pedestrians (US, 2006–2012). Almost half of the accidents occur at intersections and with no crash avoidance manoeuvres [3]. Other studies show a total of 1,819 accidents (US, 1991–1995) between WCUs and motor vehicles, nine of which were fatal [4] and 9,348 accidents where 89.2 % (US, 2002–2010) occurred in traffic on public roadways [5]. A threefold increase in the amount of powered mobility device (PMD) related accidents was found (Sweden, 2007–2016), mostly occurring at junctions or intersections. 67 % of the collisions involved cars, trucks or buses as collision partners [2]. A study focusing on motorised mobility scooters (MMS) showed that most deaths (88.3 %) resulted from collisions with motor vehicles or falling from the MMS (Australia, 2000–2011)[6]. It is yet unclear, if WCUs differ from healthy pedestrians during vehicle collision regarding kinematics, injury severity and injury locations due to a different posture and centre of mass, which might be relevant for future European New Car Assessment Programme (EURO NCAP) testing based on impactors, dummies and human body model (HBM) simulations. Current test methods only include adult and child pedestrians without disabilities in terms of pedestrian safety [7,8]. This study presents a first vehicle-to-WCU impact, with a comparison to vehicle-to-pedestrian impact based on numerical collision simulations using LS-DYNA.

II. METHODS

For the pedestrian simulation, the Total HUman Model for Safety (THUMS) AM50 Version 4.02 Pedestrian NoFracture (THUMS V4) was used [9], while for the WCU simulation, THUMS AM50 Version 5.01 Occupant NoFracture without muscle activity (THUMS V5) was used [10]. THUMS V4 has previously been validated for collision with a sedan front end structure against postmortem human subject (PMHS) test data [11]. Existing validation of THUMS V5 comprises frontal, side and rear impacts for occupant load cases [10,12], but not VRU applications. Currently, no experimental PMHS or dummy WCU data are available for validation or comparison to the best knowledge of the authors. A non-braking collision, being the second most frequent pre-crash phase manoeuvre [13], with a Toyota Yaris course model [14] was simulated at 30 km/h. The THUMS V4 previously showed the most robust model behaviour at 30 km/h [15]. The same velocity-robustness dependency was found in the early stages of this work for the THUMS V5, allowing a maximum collision speed of 30 km/h.

Injuries were predicted based on the assumption that the accumulation of effective plastic strain (over 290 ms) exceeding a threshold of 3 % in cortical bone elements results in fractures [16].

III. INITIAL FINDINGS

Data on body kinematics, resultant contact force, HIC₁₅ and cortical bone fracture prediction are presented and compared for pedestrian and WCU simulations; and to literature, if a reasonable comparison is possible. Analysis of body kinematics (Fig. 1) shows that the pedestrian is rather smoothly bending around the bodywork, while the WCU kinematics seem more abrupt due to vehicle impact. Head impact occurs at different points in time and locations for the pedestrian (185 ms, windshield) and the WCU (147 ms, hood), which is confirmed via

the resultant contact force-diagram (Fig. 2). Kinematics of the pedestrian are in compliance with literature [11] that uses a larger sedan front end structure resulting in a head impact at the upper end of the hood, compared to the windshield impact of this study.

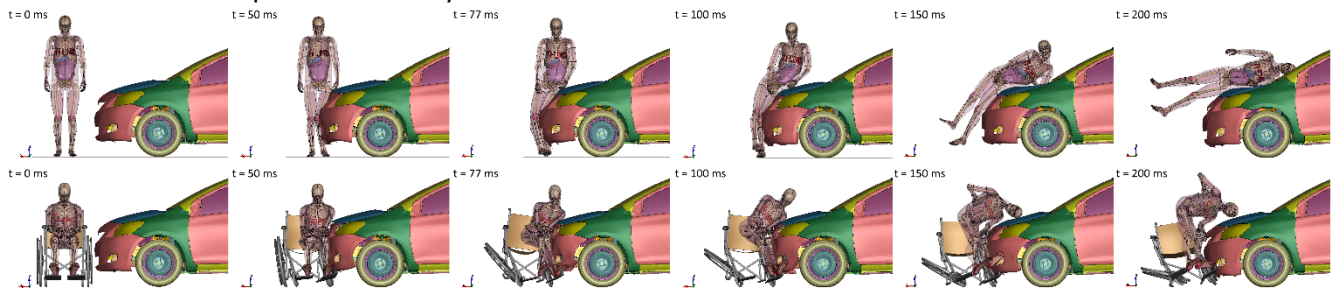


Fig. 1: Comparison of pedestrian and wheelchair user kinematics. Anterior view. Muscle elements are blanked.

Resultant force over time is shown in Fig. 2. For WCU impact, two curves are shown due to collision with the wheelchair (black, solid) and the car (red, dotted), while the pedestrian only collides with the car (blue, dashed). Peaks in resultant contact forces between the WCU and the wheelchair occurred during impact to the left ribs, arm and hip (49 ms, 10.2 kN) and left knee and elbow (136 ms, 2.4 kN). Peaks for the WCU and car contact (bumper and hood) occurred during impact to the left upper arm and knee (58 ms, 3.9 kN), left shoulder, upper arm, knee and lower leg (77 ms, 4.6 kN) and the head (147 ms, 1.5 kN). Peak contact forces for the pedestrian occurred during impact to the left upper leg and knee (40 ms, 6.1 kN), entire left leg (55 ms, 9.5 kN), entire left leg and hip (67 ms, 7.6 kN) and the head (185 ms, 6.7 kN). Peak head impact force of the pedestrian to the windshield is slightly higher than in literature [11], that found 6 kN peak head contact force to the hood at 30 km/h, due to collision with the stiffer structure.

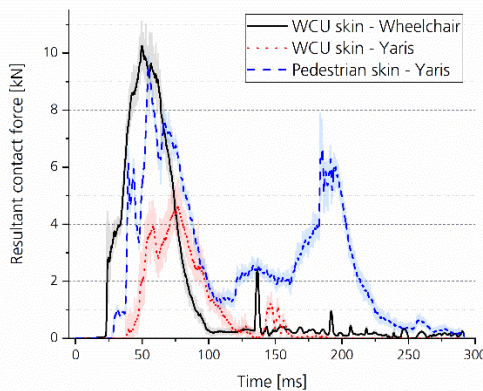


Fig. 2: Resultant contact force over time. Lines are smoothed by averaging 100 adjacent points of original data (transparent, 10 kHz output frequency) for each data point of the smoothed curves to address numerical noise.

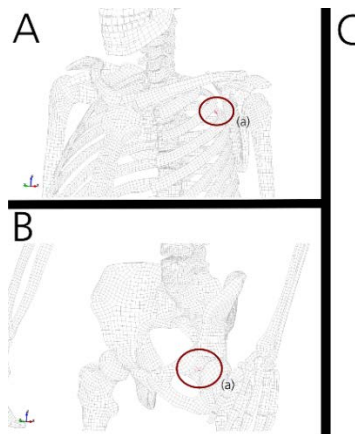


Fig. 3: Cortical bone elements with effective plastic strain greater than 3 % accumulated over 290 ms calculation time, where the primary impact occurred. Pedestrian results are shown in A and B, where the threshold was exceeded for elements in the rib and acetabulum. WCU results are shown in C, where elements in the vertebrae (a,c,j), ribs (b,e,f,g,h), radius (d) and femur (k) exceeded the threshold.

Regarding injury prediction, Fig. 3 shows that the threshold of 3 % [16] effective plastic strain is exceeded for more regions for the WCU (C) than for the pedestrian (A,B). The HIC₁₅ value, calculated for the centre of gravity of the head, is higher for the pedestrian ($HIC_{15}=455$) than for the WCU ($HIC_{15}=57$), but neither exceeds the threshold of $HIC_{15} \leq 1000$ [17].

IV. DISCUSSION

This study shows the general possibility of WCU safety analysis using state-of-the-art HBMs. Based on simulation results, a different kinematic and injury outcome can be expected for WCUs and pedestrians. A comparison of effective plastic strain to principal strain evaluation might be of interest using DYNAsaur for efficient post-processing [18]. Based on HIC₁₅ and contact force data, pedestrians have a higher risk of head injuries than WCUs. For holistic head and neck injury prediction, rotational accelerations will be considered in the future, which might play a more critical role for WCUs (Fig. 1), while HIC₁₅ might underestimate head injuries. Impact of the WCU to the stiffer wheelchair frame (steel) leads to higher contact force and might be the reason for the predicted higher fracture distribution compared to the pedestrian that was only in contact with the softer Yaris bumper (plastic) and hood (aluminium). Therefore, different material combinations for crash relevant

structures of PMDs or MMSs might be essential to mitigate peak loading and to reduce injury risk for WCUs during accidents. As no experimental PMHS data for WCU safety is currently available, this work is limited by a lack of validation of the THUMS V5 for VRU applications. Experimental crashes using biofidelic dummies are planned for future comparison. In this context, the wheelchair model will be validated. To avoid possible effects originating from different mesh sizes, THUMS V4 (pedestrian and occupant model) could be used for simulations of both VRU types in the future.

V. REFERENCES

- [1] World Health Organisation, 2018.
- [2] Carlsson A. et al., Traffic Inj Prev, 2019.
- [3] Kraemer J. D et al., BMJ Open, 2015.
- [4] NHTSA, ResearchNote, 1997.
- [5] Kraemer J. D, Inj Prev, 2015.
- [6] Kitching F. A et al., Int J Inj Contr Saf Prom, 2016.
- [7] EuroNCAP, PedTestProt, 2018.
- [8] Klug C. et al., EuroNCAP TB024, 2019.
- [9] Shigeta K. et al., ESV, 2009.
- [10] Iwamoto M. et al., Traffic Inj Prev, 2015.
- [11] Watanabe R. et al., Stapp Car Crash J, 2012.
- [12] Iwamoto M. et al., Stapp Car Crash C, 2015.
- [13] Berg A. et al., ICRASH, 2012.
- [14] NCAC., Technical Summary, 2011.
- [15] Wen L. et al., 10th European LS-DYNA C, 2015.
- [16] McCalden R. W et al., J Bone Joint Surg, 1993.
- [17] EEVC, Working Group 17 Report, 1998.
- [18] Klug C. et al., carhs HuMo, 2018.